

# Transition probabilities and lifetimes in singly ionized rhenium

P. Palmeri,<sup>1</sup> P. Quinet,<sup>1,2</sup> É. Biémont,<sup>1,2\*</sup> H. L. Xu<sup>3</sup> and S. Svanberg<sup>3</sup>

<sup>1</sup>*Astrophysique et Spectroscopie, Université de Mons-Hainaut, B-7000 Mons, Belgium*

<sup>2</sup>*IPNAS, Université de Liège, Sart Tilman B15, B-4000 Liège, Belgium*

<sup>3</sup>*Department of Physics, Lund Institute of Technology, PO Box 118, S-221 00 Lund, Sweden*

Accepted 2005 July 5. Received 2005 June 22; in original form 2005 May 12

## ABSTRACT

Transition probabilities and radiative lifetimes have been obtained for 45 transitions of Re II using a combination of radiative lifetime values obtained with the laser-induced fluorescence technique (seven levels) and theoretical branching fractions. This new set of results, concerning ultraviolet and visible lines, will be useful in the future for investigating the composition of chemically peculiar stars.

**Key words:** atomic data – atomic processes – stars: chemically peculiar

## 1 INTRODUCTION

There have been, during the past few years, strong motivations for investigating the abundances of heavy elements in chemically peculiar stars in relation to their interest for nucleosynthesis. The high-resolution ultraviolet (UV) spectra of some stars, e.g. the HgMn-type star  $\chi$  Lupi (HD 141556), made available with the *Hubble Space Telescope* Goddard High Resolution Spectrograph (GHRS), have given a strong impulse to the analysis of the chemical composition of such stars (Wahlgren et al. 1997).

Among the heavy elements of the periodic table, rhenium has been little investigated in stellar spectra. This is directly related to the rather poor knowledge of the energy level structures of Re I and Re II and to the lack of radiative data. In addition, many Re II lines are occurring in the far-ultraviolet region where little observational material was available until recently.

Nevertheless, rhenium has been detected in some chemically peculiar stars: Re I was observed in 73 Dra by Guthrie (1972) and in HD 25354 by Jaschek & Brandi (1972), and Re II in HR 465 by Bidelman, Cowley & Iler (1995). More recently, the Re II UV 1 multiplet was analysed with details by Wahlgren et al. (1997) but the weakness of the Re II feature at 227.5253 nm only allowed the determination of an upper limit to the rhenium abundance in the  $\chi$  Lupi star. Up to now, rhenium has not been identified in the photospheric solar spectrum (Asplund, Grevesse & Sauval 2005).

In the present paper we extend the set of lines usable for stellar abundance determinations by providing new atomic data for 45 UV transitions of Re II. The transition probabilities are deduced from a combination of lifetime measurements for seven levels of Re II obtained using the method of laser-induced fluorescence and theoretical branching fractions for the lines depopulating the levels of interest. These last ones have been obtained through a Hartree–Fock approach taking relativistic and core-polarization effects into account.

This method has appeared successful in recent years for obtaining transition probabilities for many heavy atoms or ions belonging particularly to the lanthanide group (see, for example, the data base DREAM and the references therein at <http://w3.umh.ac.be/~astro/dream.shtml>).

## 2 ATOMIC STRUCTURE AND SPECTRUM OF RE II

Terrestrial rhenium consists of two stable isotopes <sup>185</sup>Re (37.5 per cent) and <sup>187</sup>Re (62.5 per cent), each isotope having a nuclear spin  $I = 5/2$ .

The ground-state level of Re II is  $5d^5(^6S)6s a^7S_3$  and the first excited experimentally determined configurations are  $5d^4 6s^2$ ,  $5d^5(^4D, ^6S, ^4G)6s$ ,  $5d^6$ ,  $5d^5 6p$  and  $5d^4 6s 6p$ . The most comprehensive rhenium analysis published to date is due to Meggers (1952) using arc and spark laboratory data. About 1000 classified lines of Re II have been published (Meggers, Catalan & Sales 1958) covering the wavelength range extending from 152.5 up to 1160 nm. Many of these transitions are affected by hyperfine structure effects and by isotope shifts.

Transition probabilities in Re II are very scarce. The first results were the arc measurements of Corliss & Bozman (1962), but it is now well established that they contain large systematic errors. More recently, some lifetime measurements have been published by Wahlgren et al. (1997) and by Henderson et al. (1999) but they concern only the two  $z^7P_{2,3}^0$  levels. A compilation of wavelengths of Re II (longward of the Lyman limit) has also been proposed by Morton (2000, 2001).

## 3 EXPERIMENTAL METHOD

Radiative lifetimes of seven levels belonging to the  $(5d+6s)^5 6p$  strongly mixed complex (odd parity) were measured using the time-resolved laser-induced fluorescence (LIF) technique. The experimental set-up used in the lifetime measurements has been previously

\*E.Biémont@ulg.ac.be

**Table 1.** Odd-parity levels measured in Re II and the corresponding excitation schemes.

$E$ (cm <sup>-1</sup> ) <sup>a</sup>	$J$	Origin	Excitation $\lambda_{\text{air}}$ (nm)	Laser mode <sup>c</sup>	Observed $\lambda_{\text{air}}$ (nm)
43 937.578 <sup>b</sup>	2	0.0	227.53	$3\omega + S$	337
45 147.445 <sup>b</sup>	3	0.0	221.42	$3\omega$	330
49 439.3	1	13 777.3	280.33	$2\omega + A$	310
52 677.0	2	14 352.2	260.85	$3\omega + 2S$	282
53 802.1	3	14 352.2	253.41	$3\omega + 2S$	273
57 050.2	3	14 882.6	237.08	$3\omega + S$	264
57 138.6	2	14 930.5	236.85	$3\omega + S$	296

<sup>a</sup>Meggers et al. (1958). <sup>b</sup>Wahlgren et al. (1997). <sup>c</sup> $2\omega$  and  $3\omega$  designate the second and third harmonics of the dye laser, and 2S and 2A represent the second-order Stokes and anti-Stokes components.

illustrated (see, for example, Biémont et al. 2002, 2003; Xu et al. 2003a,c,d). The Re<sup>+</sup> ions are generated in a laser-produced plasma. The excitation radiation used in this experiment had a pulse duration of 1 ns, which was obtained by sending a frequency-doubled Nd:YAG laser with 8-ns duration into a stimulated Brillouin scattering (SBS) cell filled with pure water. These pulses were used to pump a dye laser. The excitation process was performed in a vacuum chamber with a background pressure of  $10^{-6}$ – $10^{-5}$  mbar. For more details, see Biémont et al. (2004) and Xu et al. (2004).

The levels measured in the present work and the excitation schemes are shown in Table 1. As mentioned, the ground state of Re II is  $5d^5(6S)6s\ a^7S_3$ . The  $z^7P_{2,3}^0$  levels were directly populated from the ground state through a single-step excitation process; the other five levels were excited from four metastable states belonging to  $5d^46s^2$ ,  $5d^5(^4D)6s$  and  $5d^6$  configurations, respectively. The populations of the metastable states result from the recombination of electrons and ions in the laser-produced plasma and possible cascade decays of high-lying excited states (see, for example, Xu et al. 2003b). As can be seen in Table 1, the achievement of the Re II ions in the metastable states makes the lifetime measurements feasible for some high-lying Re II levels by using the excitation light in the UV spectral region; otherwise, the excitation wavelengths for these levels would fall into the vacuum ultraviolet (VUV) range, which is generally technically more complicated (Li et al. 2000). The laser mode in Table 1 shows different non-linear generation processes used in the experiment. The numbers 2 and 3 designate the second and third harmonics of the radiation from the dye laser. S, 2S and A represent the first-order, second-order Stokes and first-order anti-Stokes components of the harmonics in a Raman cell filled with  $H_2$  gas (Biémont et al. 2004).

The last column of Table 1 shows the observed wavelengths, which are different from the excitation channels for all the levels under investigation in order to avoid the scattered light originating from the excitation beam (see further below).

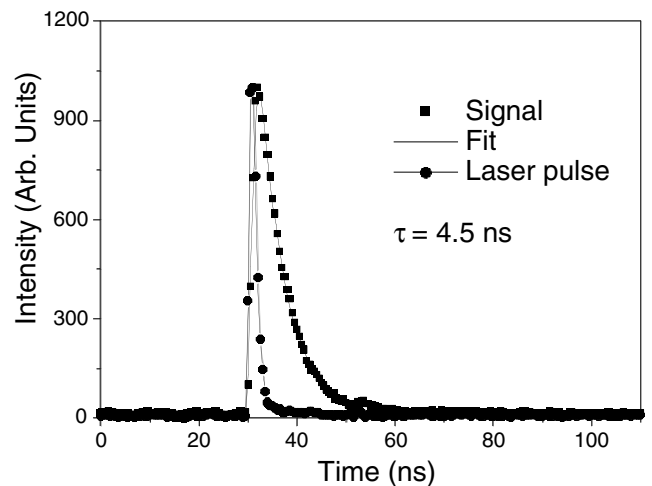
In the measurements, the effects of cascades from excited states on the measured radiative lifetimes could be excluded because the measurements were performed generally with the delay time of 3–7  $\mu$ s between the ablation and excitation lasers. A 3- $\mu$ s delay before the measurements is long enough to allow all ions in high-lying excited states to decay. This can be confirmed by observing the background without applying the excitation light. No background fluorescence could be observed with the delay time between 3 and 7  $\mu$ s.

In the measurements, attention has also been paid to several other systematic effects, such as flight-out-of-view effects and quantum

beat effects, which can potentially affect the lifetime values. To make sure that the experimental lifetimes were not affected by collisional quenching and radiation trapping, measurements were performed under different plasma conditions, i.e. by varying the density and temperature of the plasma and the ion speed, which can be adjusted by changing the intensity of the ablation pulse, the size of the focused ablation pulse spot and the delay time between the ablation and excitation pulses. Consequently, the intensities of fluorescence signals were varied by a factor of 5, but the lifetime values were found to be constant. This implied that collisional quenching and radiation trapping effects were negligible.

We have also taken into account the quantum beats on the decay curves due to the Zeeman effect. It is well known that a strong magnetic field over the interaction area will change the duration of the Larmor precession of ions. Therefore, the fluorescence decays were recorded in the absence and in the presence of an external magnetic field of about 100 G, which was provided by a pair of Helmholtz coils. In the present experiment, no effects due to quantum beats were observed. Flight-out-of-view effects were also considered during the measurements by adjusting the delay time between the ablation and excitation pulses, which determined the speed of the Re II ions when the distance of the excitation beam and the sample target was fixed (10 mm). With a delay time of 5  $\mu$ s, the velocities of Re II ions in the interaction area were about 2 km s<sup>-1</sup>. For the lifetime of the level at 49 439.3 cm<sup>-1</sup> (17.8 ns), it was found desirable to observe the decay signal within 71.4 ns, i.e. four times the lifetime. The ion flight distance was then 0.15 mm along the direction of the ion movement. In the experiment, the entrance slit of the monochromator was chosen between 0.6 and 3 mm. Therefore, the flight-out-of-view effects can be considered to be negligible.

For the level at 49 439.3 cm<sup>-1</sup>, the lifetimes were evaluated with exponential fitting processes applied to the decays after the excitation pulse, which gives a lifetime of 17.8 ns. For other levels, the lifetime results were obtained by a deconvolution process, as shown in Fig. 1. The time-resolved signal is a convolution of a pure exponential curve with the temporal shape of the excitation pulse. In the deconvolution process, it is very important to avoid saturation effects; therefore, the fluorescence signals were detected with different neutral density filters inserted in the exciting light path during the experiment. Another important aspect in the deconvolution process is to avoid the background due to the scattered light of excitation


**Figure 1.** A typical decay curve for the  $z^7P_2^0$  level of Re II, with a convolution fit.

**Table 2.** Comparison between calculated and experimental radiative lifetimes (in ns) in Re II.

$E$ (cm <sup>-1</sup> ) <sup>a</sup>	$J$	LS-coupling composition <sup>c</sup>	Calculation This work	Experiment This work	Experiment Other studies
43 937.578 <sup>b</sup>	2	69 A(6S)7P <sup>o</sup> + 9 A(6S)5P <sup>o</sup> + 6 A(4P)5P <sup>o</sup> + 5 B(5D)7P <sup>o</sup>	3.98	4.5 ± 0.3	4.47 ± 0.2 <sup>b</sup> 5.1 ± 0.8 <sup>d</sup>
45 147.445 <sup>b</sup>	3	55 A(6S)7P <sup>o</sup> + 19 A(6S)5P <sup>o</sup> + 6 A(4P)5P <sup>o</sup> + 4 A(4P)5D <sup>o</sup>	4.03	4.6 ± 0.3	6.7 ± 0.8 <sup>d</sup>
49 439.3	1	26 B(5D)7D <sup>o</sup> + 21 B(5D)5P <sup>o</sup> + 18 B(5D)7F <sup>o</sup> + 8 B(3P)5P <sup>o</sup>	17.39	17.8 ± 1.5	
52 677.0	2	21 A(6S)5P <sup>o</sup> + 16 B(5D)7D <sup>o</sup> + 14 A(6S)7P <sup>o</sup> + 10 B(5D)5P <sup>o</sup>	4.46	4.2 ± 0.3	
53 802.1	3	31 A(6S)5P <sup>o</sup> + 27 A(6S)7P <sup>o</sup> + 9 A(4P)3D <sup>o</sup> + 7 B(5D)7P <sup>o</sup>	3.98	3.4 ± 0.3	
57 050.2	3	18 B(5D)7P <sup>o</sup> + 7 B(5D)7D <sup>o</sup> + 6 A(4G)5H <sup>o</sup> + 6 A(4G)5G <sup>o</sup>	3.73	6.5 ± 0.4	
57 138.6	2	27 B(5D)7P <sup>o</sup> + 7 A(4D)5F <sup>o</sup> + 7 A(4P)5D <sup>o</sup> + 6 A(6S)7P <sup>o</sup>	4.88	8.3 ± 0.5	

<sup>a</sup>Meggers et al. (1958). <sup>b</sup>Wahlgren et al. (1997). <sup>c</sup>The four major components are given in per cent. A and B stand for 5d<sup>5</sup>6p and 5d<sup>4</sup>6s6p, respectively. <sup>d</sup>Henderson et al. (1999).

beam, which will cause the lifetime values to become smaller. We thus chose the observation channels different from the excitation wavelengths, as shown in Table 1. Fluorescence signals in the different decay channels, from excited upper levels to possible lower levels, were checked in order to ensure that the Re II transitions of interest were indeed studied.

All experimental lifetime results are summarized in Table 2 where they are compared with previous experimental results as well as with the theoretical values calculated in this work (see further below). The error bars of the values in Table 2 were determined from the statistical spread of the different curve recordings.

As can be seen in Table 2, the lifetime value (4.5 ns) of the z<sup>7</sup>P<sub>2</sub><sup>o</sup> level is in good agreement with the LIF measurement combined with a hollow cathode discharge lamp by Wahlgren et al. (1997). However, the lifetime values of z<sup>7</sup>P<sub>2,3</sub><sup>o</sup> levels measured in this work are systematically smaller than the results obtained by Henderson et al. (1999) using the beam foil method. As discussed by Henderson et al. (1999), the measurement of the z<sup>7</sup>P<sub>2</sub><sup>o</sup> level in Re II has larger error bars because the Re II lines might possibly be affected by cascade repopulation.

#### 4 CALCULATIONS

The spectroscopic term analysis in Re II due to Meggers et al. (1958) was based on the arc and spark spectra recorded and published 6 yr earlier (Meggers 1952). Using observed Zeeman patterns for 220 Re II lines, they found 49 even and 85 odd levels that classified 1040 lines and determined the ground state to be 5d<sup>5</sup>(a<sup>6</sup>S)6s<sup>2</sup>7S<sub>3</sub>. A revision of the even parity term analysis was realized by Wyart (1977) who carried out the first parametric study of the low-lying even configurations 5d<sup>5</sup>6s, 5d<sup>4</sup>6s<sup>2</sup> and 5d<sup>6</sup>. The levels at 22 031, 23 381, 27 627, 32 206 and 36 993 cm<sup>-1</sup> were excluded from the least-squares fitting procedure. The first three levels were considered as determined from accidental coincidences and the last two were assigned wrong  $J$  quantum numbers. Wyart proposed a new level at 20 781.5 cm<sup>-1</sup> with  $J = 6$ . No additional revision of the interpretation of the Re II spectrum has been attempted to our knowledge since then.

The measurement of the hyperfine structure and isotope shifts of the three resonance transitions a<sup>7</sup>S<sub>3</sub>-z<sup>7</sup>P<sub>2,3,4</sub><sup>o</sup> was carried out by Wahlgren et al. (1997).

In the present calculations, we used the pseudo-relativistic Hartree-Fock (hereafter HFR) method of Cowan (1981) to determine theoretical values of the radiative lifetimes measured here. For such a heavy element ( $Z = 75$ ), both core-valence and valence-

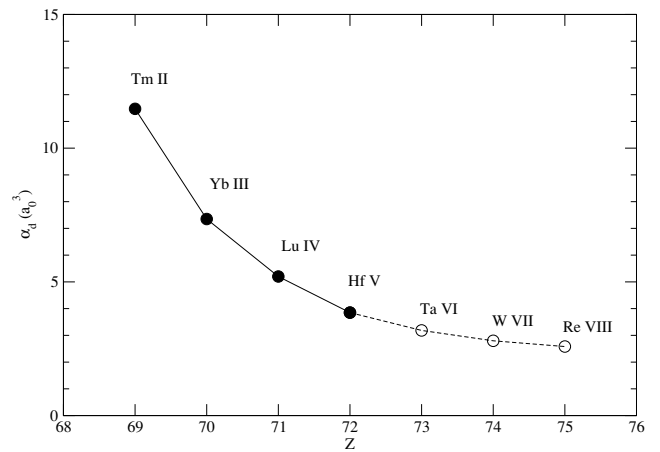


**Figure 2.** Static dipole polarizability,  $\alpha_d$ , in  $a_0^3$  versus the atomic number,  $Z$ , along the erbium isoelectronic sequence. Filled circles denote values tabulated in Fraga et al. (1976), and open circles are extrapolated values.

valence correlations have to be taken into account alongside relativity.

In order to do so, the core-valence correlations have been modelled using a core-polarization potential and a correction to the electric dipole transition operator, as described in detail in our earlier studies (see, for example, Quinet et al. 1999). A 4f<sup>14</sup> erbium-like ionic core surrounded by six valence electrons has been chosen. As the dipole polarizability was not tabulated in Fraga, Karwowski & Saxena (1976), a value of 2.58  $a_0^3$  has been extrapolated along the isoelectronic sequence, as shown in Fig. 2. The HFR value for the mean radius of the outermost core orbital, i.e. 5p, has been used for the cut-off radius. Concerning the valence-valence correlations, we considered explicitly the interactions between the following configurations: 5d<sup>5</sup>ns, 5d<sup>4</sup>6sns, 5d<sup>6</sup>, 5d<sup>5</sup>6d, 5d<sup>4</sup>6s6d, 5d<sup>3</sup>6s<sup>2</sup>6d, 5d<sup>4</sup>6p<sup>2</sup> and 5d<sup>3</sup>6s6p<sup>2</sup> with  $n = 6-8$  for the even parity; 5d<sup>5</sup>np, 5d<sup>4</sup>6snp and 5d<sup>3</sup>6s<sup>2</sup>6p with  $n = 6-8$  for the odd parity.

A 0.8 scaling factor has been applied to the Slater integrals according to a well-established practice (see, for example, Biémont et al. 2002, 2003; Xu et al. 2003a,b,c,d) in order to consider the effect of far-interacting configurations non-explicitly included.

The radial parameters representing the electrostatic and spin-orbit interactions within and between the configurations 5d<sup>5</sup>6s, 5d<sup>4</sup>6s<sup>2</sup>, 5d<sup>6</sup>, 5d<sup>5</sup>6p and 5d<sup>4</sup>6s6p have been adjusted so as to improve the agreement between the eigenvalues and the available experimental energy levels (Meggers et al. 1958; Wyart 1977; Wahlgren et al.

**Table 3.** Weighted transition probabilities (gA) ( $10^7 \text{ s}^{-1}$ ), branching fractions (BF), observed intensities and Landé factors (g) for the strongest lines depopulating the odd levels for which lifetime measurements have been performed.

$E_{\text{upp}}^a$ ( $\text{cm}^{-1}$ )	$J$	$E_{\text{low}}^a$ ( $\text{cm}^{-1}$ )	$J'$	$\lambda^c$ (nm)	$gA_{\text{calc}}^d$	$BF_{\text{calc}}^e$	$CF^f$	$BF_{\text{exp}}^b$	$gA_{\text{exp}}^g$	Arc Int. <sup>h</sup>	Spark Int. <sup>i</sup>	$g_{\text{calc}}^e$ Upp. Low.	$g_{\text{exp}}^a$ Upp. Low.				
43 937.578 <sup>b</sup>	2	0.0	3	227.525	103	0.928	0.40	$0.60 \pm 0.04$ 0.20 <sup>j</sup>	280	5200	500	2.187	1.979	2.19	2.05		
		14352.2	2	337.908	4	0.038	0.17		220	320	100		1.533		1.53		
		17223.5	2	374.228	1	0.011	0.07		99	130	200		1.715		1.71		
45 147.445 <sup>b</sup>	3	0.0	3	221.427	130	0.855	0.41		150	4200	1000	1.788	1.979	1.79	2.05		
		17223.5	2	358.013	10	0.067	0.27		820	810	300		1.715		1.71		
		14882.6	4	330.321	6	0.039	0.12		300	320	50		1.483		1.48		
		14930.5	3	330.845	3	0.018	0.06				5		1.486		1.48		
		14352.2	2	324.632	2	0.011	0.05				80		1.533		1.53		
49 439.3	1	17223.5	2	310.317	7	0.436	-0.16		360	140	40s	2.318	1.715	2.42	1.71		
		14824.0	1	288.805	4	0.259	-0.10		290	130	40		1.506		1.50		
		13777.3	0	280.328	3	0.157	0.10		260	120	20		0/0		0/0		
52 677.0	2	0.0	3	189.836	44	0.366	-0.24				100	1.811	1.979	1.82	2.05		
		14352.2	2	260.850	41	0.345	0.21		2200	660	400		1.533		1.53		
		17223.5	2	281.977	8	0.069	0.05		280	75	60		1.715		1.71		
		19139.7	3	298.088	7	0.062	0.12				50		1.104		1.12		
		14824.0	1	264.101	6	0.048	-0.11		300	90	30		1.506		1.50		
		21629.1	3	321.990	6	0.047	-0.09				50		1.276		1.26		
		14930.5	3	264.846	1	0.013	-0.01		220	65	50		1.486		1.48		
		22544.7	2	331.774	1	0.013	0.02				15		1.224		1.20		
		53 802.1	3	0.0	3	185.866	67	0.326	-0.15				200	1.657	1.979	1.66	2.05
17223.5	2			273.303	48	0.232	0.22		2430	610	300		1.715		1.71		
14882.6	4			256.864	42	0.203	0.22		1830	540	300		1.483		1.48		
14930.5	3			257.180	27	0.132	0.22		1250	370	300		1.486		1.48		
14352.2	2			253.410	12	0.058	0.07		490	150	80		1.533		1.53		
27746.0	3			383.678	1	0.006	-0.03				20		1.227		1.23		
57 050.2	3	0.0	3	175.284	62	0.573	0.48				18	1.321	1.979	1.135	2.05		
		14882.6	4	237.076	10	0.092	0.10		370	220	100		1.483		1.48		
		19139.7	3	263.701	9	0.086	-0.07		990	190	150		1.104		1.12		
		18845.8	2	261.672	8	0.075	-0.09		810	160	150		0.631		0.64		
		14930.5	3	237.346	8	0.071	-0.04		260	150	50		1.486		1.48		
		24763.1	3	309.631	3	0.027	-0.04				15		1.422		1.41		
		26237.3	4	324.446	2	0.015	0.04				15		1.124		1.12		
		23340.8	2	296.567	2	0.014	-0.03						1.679		1.67		
		22544.7	2	289.724	1	0.012	0.02					10		1.224		1.20	
		20463.2	4	273.240	1	0.010	-0.03					6		1.174		1.18	
		57 138.6	2	0.0	3	175.013	34	0.566	-0.54				200	1.335	1.979	1.30	2.05
				19139.7	3	263.087	5	0.080	-0.06				30		1.104		1.12
14352.2	2			233.647	4	0.071	0.02				15		1.533		1.53		
23340.8	2			295.791	4	0.070	0.07		790	130	80		1.679		1.67		
23146.2	1			294.097	3	0.054	0.06				50		1.144		1.10		
17223.5	2			250.456	3	0.044	-0.03		1060	230	30		1.715		1.71		
14930.5	3			236.849	2	0.031	0.02		320	180	50		1.486		1.48		
22544.7	2			288.984	1	0.013	0.01				10		1.224		1.20		
18845.8	2			261.068	1	0.012	-0.02				20b?		0.631		0.64		
14824.0	1			236.253	1	0.012	0.01				10		1.506		1.50		

<sup>a</sup>Meggers et al. (1958). Landé factors in parentheses are mean values from resolved Zeeman patterns adopted to compute the other g values from unresolved patterns (Meggers et al. 1958). <sup>b</sup>Wahlgren et al. (1997). <sup>c</sup>Calculated in the air (above 200 nm) from the experimental energy levels. <sup>d</sup>Determined by combining the present measured lifetimes with the calculated BF. <sup>e</sup>This work. <sup>f</sup>Cancellation factor. Absolute values less than 0.05 indicate calculated line strengths affected by strong cancellation effects (Cowan 1981). <sup>g</sup>Corliss & Bozman (1962). <sup>h</sup>Line intensities in the arc spectra of Meggers et al. (1975). <sup>i</sup>Line intensities in the spark spectra of Meggers (1952) and Meggers et al. (1958). s denotes sum of two contributions, and b? a possible blend. <sup>j</sup>Estimated using the  $\lambda\lambda 2275.25, 3379.06$  line ratio measured by Wahlgren et al. (1997).

1997) using the least-squares fit procedure implemented in the RCE program (Cowan 1981). 44 even-parity and 55 odd-parity experimental levels have been included in the fitting process. The standard deviations were 135 and 192  $\text{cm}^{-1}$  for the even and odd parities, respectively. We have excluded from the fit the same five even levels as in Wyart (1977) and all the odd levels above 70 000  $\text{cm}^{-1}$  along with five odd levels below 70 000  $\text{cm}^{-1}$ , i.e. the levels at 54 468, 64 966, 66 536, 68 354 and 69 302  $\text{cm}^{-1}$ . The level at 54 468  $\text{cm}^{-1}$ , which is interpreted as  $5d^46s(^6D)6p z^5D_0$  by Meggers et al. (1958), is determined by only three weak coincidences among which two are doubly classified lines. The closest theoretical odd level with

$J = 0$  is predicted at 55 742  $\text{cm}^{-1}$ , which seems too far compared to the standard deviation. Regarding the three  $J = 3$  levels at 64 966, 68 354 and 69 302  $\text{cm}^{-1}$  and the  $J = 5$  level at 66 536  $\text{cm}^{-1}$ , there are no more eigenvalues left in our respective energy matrices that can correspond to them. Moreover, they are all determined with less than eight weak lines. Eight coincidences can be considered as a threshold below which they could be statistically accidental, as explained in detail in Meggers et al. (1958).

In Table 2, we compare our calculated lifetimes with our experimental values and with the LIF measurements of Wahlgren et al. (1997) and Henderson et al. (1999). The atomic state compositions

are given here showing the strong mixing between the configurations  $5d^56p$  and  $5d^46s6p$  and the departures from the LS coupling scheme. Indeed, the levels at 43 937 and 45 147  $\text{cm}^{-1}$  appear with a major LS component of 69 per cent  $5d^5(^6S)6p\ ^7P_2^0$  and 55 per cent  $5d^5(^6S)6p\ ^7P_3^0$ , respectively, in contradistinction to the designations proposed by Meggers et al. (1958), but in accord with those given in the tables of Moore (1958). Concerning the other levels, they have all major components with less than 35 per cent rendering any LS-designation attempt highly hazardous. Concerning the radiative lifetimes, our calculations agree with our measurements within 20 per cent if we put aside the last two levels at 57 050 and 57 138  $\text{cm}^{-1}$  for which there is a 40 per cent disagreement. Regarding these last two levels, it can be noticed that the four major components describe less than 50 per cent of the atomic states. In fact, their calculated lifetimes were found to be very sensitive to the fitting procedure in comparison to the others. The lifetime measured by Henderson et al. (1999) for the level at 45 147  $\text{cm}^{-1}$  seems too long according to our experiment and to our calculations.

Table 3 shows the weighted transition probabilities (gA), branching fractions (BF), observed arc (Meggers, Corliss & Scribner 1975) and spark intensities (Meggers 1952; Meggers et al. 1958) and Landé factors (g) for the strongest lines depopulating the seven odd-parity levels reported in Table 2. The calculated gA values presented here have been obtained by combining our measured lifetimes with our calculated BF values. Most of the decay channels of the levels at 57 050 and 57 138  $\text{cm}^{-1}$  have their line strengths affected by strong cancellation effects (Cowan 1981). This explains in part the sensitivity of the calculated lifetimes to the fitting process.

The comparison of our calculated gA values with the observed arc and spark intensities displays a fair agreement in terms of their relative values. Important disagreements in absolute and, in some instances, in relative values are found when we compare them with the transition probabilities determined by Corliss & Bozman (1962). The experimental BF values of Wahlgren et al. (1997) are in significant discord with our calculations. For such strong transitions, self-absorption can be an issue, making the resonance line appear weaker with respect to the other decay channels. However, Wahlgren et al. (1997) reduced the direct current in their hollow cathode discharge so that the measured branching ratios became constant, and therefore made sure that their plasma was optically thin. Nevertheless, it can be noticed that the arc intensities of Meggers et al. (1975) seem to favour our calculated BF values. A comparison between the calculated and experimental Landé factors, as determined for each Zeeman pattern by Meggers et al. (1958), is also reported in this table. An excellent accord is found if we except the case of the decay channels of the level at 57 050  $\text{cm}^{-1}$ .

## 5 CONCLUSIONS

The present work extends the set of transition probabilities available in Re II. The combination of experimental radiative lifetimes measured by LIF, with calculated branching fractions obtained using a HFR approach in which core-polarization effects are included, has appeared useful for providing *f* values for 45 UV and visible transitions. This procedure has allowed us to take into account some strong depopulation branches appearing in the far-UV region whose intensities cannot be measured directly in the laboratory. It is anticipated

that these new data will help astrophysicists in the future to refine the investigation of the chemical composition of some stars when high-resolution spectra become available in these spectral regions.

## ACKNOWLEDGMENTS

This work was financially supported by the Swedish Research Council and by the EU-TMR access to Large-Scale Infrastructure Programme (contract RII3-CT-2003-506350). Financial support from the Belgian FNRS is acknowledged by two of us (EB and PQ) PP was funded by a return grant of the Belgian Federal Science Policy.

## REFERENCES

- Asplund M., Grevesse N., Sauval A. J., 2005, in Barnes T. G., III, Bash F. N., eds, ASP Conf. Ser. Vol. 336, Cosmic Abundance as Records of Stellar Evolution and Nucleosynthesis, in Honor of David L. Lambert. Astron. Soc. Pac., San Francisco, p. 25
- Bidelman W. P., Cowley C. R., Iler A. L., 1995, *Pub. Obs. Univ. Michigan*, 12 (3)
- Biémont E., Garnir H. P., Quinet P., Svanberg S., Zhang Z. G., 2002, *Phys. Rev. A*, 65, 052502
- Biémont E., Garnir H. P., Litzén U., Nielsen K., Quinet P., Svanberg S., Wahlgren G., Zhang Z. G., 2003, *A&A*, 399, 343
- Biémont E., Quinet P., Svanberg S., Xu H. L., 2004, *J. Phys. B*, 37, 1381
- Corliss C. H., Bozman W. R., 1962, *Natl. Bur. Stand. Monograph* 53. US Department of Commerce, Washington DC
- Cowan R. D., 1981, *The Theory of Atomic Structure and Spectra*. Univ. of California Press, Berkeley, CA
- Fraga S., Karwowski J., Saxena K. M. S., 1976, *Handbook of Atomic Data*. Elsevier, Amsterdam
- Guthrie B. N. G., 1972, *ApJS*, 15, 214
- Henderson M., Irving R. E., Matulioniene R., Curtis L. J., Ellis D. G., Wahlgren G. M., Brage T., 1999, *ApJ*, 520, 805
- Jaschek M., Brandt E., 1972, *A&A*, 20, 233
- Li Z. S., Lundberg H., Berzinsh U., Johansson S., Svanberg S., 2000, *J. Phys. B*, 33, 5593
- Meggers W. F., 1952, *J. Res. Natl. Bur. Stand.*, 49, 187
- Meggers W. F., Catalan M. A., Sales M., 1958, *J. Res. Natl. Bur. Stand.*, 61, 441
- Meggers W. F., Corliss C. H., Scribner B. F., 1975, *NBS Monograph* 145. US Department of Commerce, Washington DC
- Moore C. E., 1958, *Atomic Energy Levels*, Vol. III, NBS, Monograph 467. US Department of Commerce, Washington DC
- Morton D. C., 2000, *ApJS*, 130, 403
- Morton D. C., 2001, *ApJS*, 132, 411
- Quinet P., Palmeri P., Biémont E., McCurdy M. M., Rieger G., Pinnington E. H., Wickliffe M. E., Lawler J. E., 1999, *MNRAS*, 307, 934
- Wahlgren G. M., Johansson S. G., Litzén U., Gibson N. D., Cooper J. C., Lawler J. E., Leckrone D. S., Engleman R., 1997, *ApJ*, 475, 380
- Wyart J.-F., 1977, *Optica Pura y Aplicada*, 10, 177
- Xu H. L., Svanberg S., Quinet P., Garnir H. P., Biémont E., 2003a, *J. Phys. B*, 36, 4773
- Xu H. L., Svanberg S., Cowan R. D., Lefèbvre P.-H., Quinet P., Biémont E., 2003b, *MNRAS*, 346, 433
- Xu H. L., Zhankui J., Zhang Z. G., Dai Z., Svanberg S., Quinet P., Biémont E., 2003c, *J. Phys. B*, 36, 1771
- Xu H. L., Svanberg S., Quinet P., Garnir H. P., Biémont E., 2003d, *J. Phys. B*, 36, 4773
- Xu H. L. et al., 2004, *Phys. Rev. A*, 70, 042508

This paper has been typeset from a  $\text{\TeX}/\text{\LaTeX}$  file prepared by the author.